A Structure Is Worth a Thousand Words: New Insights for RAS and RAF Regulation

Dhirendra K. Simanshu[1] and Deborah K. Morrison[2]

ABSTRACT The RAS GTPases are frequently mutated in human cancer, with KRAS being the predominant tumor driver. For many years, it has been known that the structure and function of RAS are integrally linked, as structural changes induced by GTP binding or mutational events determine the ability of RAS to interact with regulators and effectors. Recently, a wealth of information has emerged from structures of specific KRAS mutants and from structures of multiprotein complexes containing RAS and/or RAF, an essential effector of RAS. These structures provide key insights regarding RAS and RAF regulation as well as promising new strategies for therapeutic intervention.

Significance: The RAS GTPases are major drivers of tumorigenesis, and for RAS proteins to exert their full oncogenic potential, they must interact with the RAF kinases to initiate ERK cascade signaling. Although binding to RAS is typically a prerequisite for RAF to become an activated kinase, determining the molecular mechanisms by which this interaction results in RAF activation has been a challenging task. A major advance in understanding this process and RAF regulation has come from recent structural studies of various RAS and RAF multiprotein signaling complexes, revealing new avenues for drug discovery.

INTRODUCTION

Mutated *RAS* genes were the first cellular oncogenes to be identified in human tumors more than 40 years ago. Through decades of research, the RAS GTPases have been established to function as molecular switches that cycle between active and inactive states to transmit signals that regulate critical cellular processes, including proliferation, migration, apoptosis, and survival (reviewed in refs. 1, 2). The conversion of RAS from the inactive GDP-bound form to the active GTP-bound state is stimulated by guanine nucleotide exchange factors (GEF), which catalyze the exchange of GDP for GTP (Fig. 1A). Active RAS is then converted back to the inactive form by GTPase-activating proteins (GAP), such as NF1 and RASA1/p120GAP, which accelerate the intrinsic GTP hydrolysis rate of RAS by five orders of magnitude. In the active state, RAS interacts with a large number of effector proteins, most notably the RAF kinases, PI3K, and RALGDS, leading to the activation of multiple downstream signaling cascades that together constitute "the RAS pathway."

Of the RAS pathway components, the structure of RAS itself was the first to be solved, and in this review, we will discuss how the structural analysis of RAS has greatly advanced our understanding of the molecular mechanisms that regulate RAS function. In addition, we will describe how recent structures of complexes containing RAS and/or RAF have provided critical insight regarding how RAS binding promotes the activation of one of its key downstream effectors, the RAF kinase family.

RAS STRUCTURE AND SWITCH REGIONS

The three human *RAS* genes encode four different RAS protein isoforms—HRAS, NRAS, KRAS4A, and KRAS4B—with the last two isoforms arising from alternative splicing of the fourth *KRAS* exon, thus generating KRAS proteins with different C-terminal sequences. Although all four RAS isoforms share high sequence and structural homology in the GTPase domain (G-domain; 1–166), they differ significantly in the last 20 amino acids, forming what is known as the RAS hypervariable region (HVR), a segment that plays a critical role in anchoring RAS to the inner leaflet of the plasma membrane. Due to its GTP-binding activity and sequence homology, the

[1]NCI RAS Initiative, Cancer Research Technology Program, Frederick National Laboratory for Cancer Research, Leidos Biomedical Research, Inc., Frederick, Maryland. [2]Laboratory of Cell and Developmental Signaling, Center for Cancer Research, National Cancer Institute, Frederick, Maryland.

Corresponding Authors: Dhirendra K. Simanshu, NCI RAS Initiative, Cancer Research Technology Program, FNL for Cancer Research, Leidos Biomedical Research, Inc., Frederick, MD 21702. Phone: 301-360-3438; E-mail: dhirendra.simanshu@nih.gov; and Deborah K. Morrison, Laboratory of Cell and Developmental Signaling, National Cancer Institute, 1050 Boyles Street, ATRF D3027, Frederick, MD 21702. Phone: 301-846-1733; E-mail: morrisod@mail.nih.gov

Cancer Discov 2022;12:899–912

doi: 10.1158/2159-8290.CD-21-1494

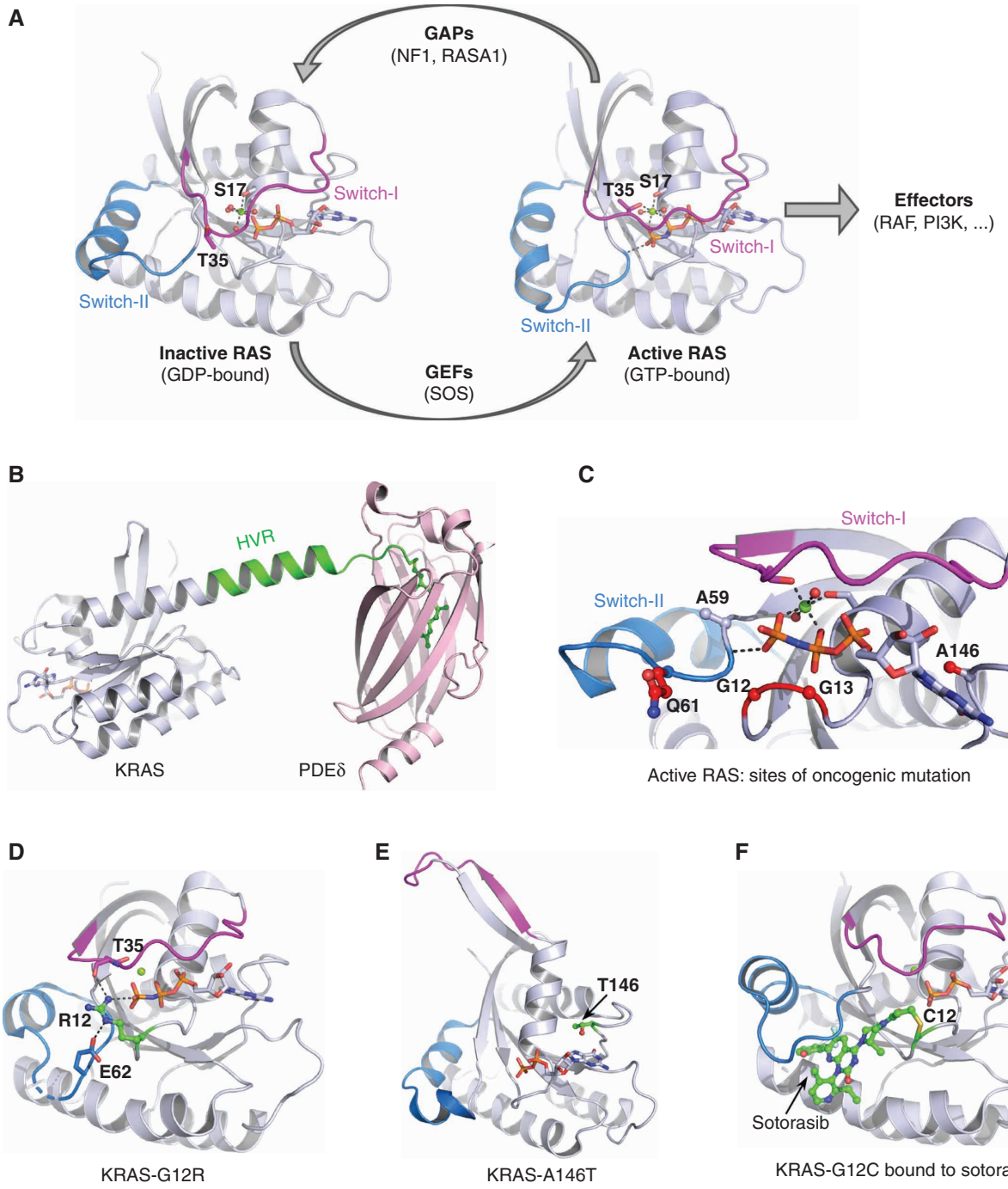

Figure 1. RAS GDP/GTP cycle and structural changes in RAS-mutant alleles. **A,** RAS cycles between inactive GDP-bound and active GTP-bound states to regulate effector-mediated signaling. Inactive RAS is activated by GDP/GTP exchange stimulated by GEFs such as SOS (Son of Sevenless). Active RAS is converted back to the inactive state by GTP hydrolysis stimulated by GAPs such as NF1 and RASA1/p120GAP. KRAS-GDP (PDB ID: 6MBT) and KRAS-GppNHp (PDB ID: 6XI7) are shown in cartoon representation, and the bound nucleotide and Mg^{2+} are shown in stick and sphere representations, respectively. Switch-I and switch-II regions are colored magenta and blue, and interactions formed by Mg^{2+} and γ-phosphate are shown using dashed lines. Side-chain atoms of S17 and T35 (only in KRAS-GppNHp) coordinate with Mg^{2+} and are shown in stick representation. **B,** Structure of full-length farnesylated and methylated KRAS4B in complex with PDEδ (PDB ID: 5TAR). In this panel, KRAS4B and PDEδ (pink) are shown in cartoon representation, whereas prenylated C185 (green) and GDP are shown in stick representation. **C,** Enlarged view of the nucleotide-binding pocket in the GppNHp-bound KRAS (PDB ID: 6XI7) showing switch regions and residues (ball and stick representation) that are mutated in RAS-driven cancers. **D** and **E,** Crystal structure of GppNHp-bound $KRAS^{G12R}$ (PDB ID: 6CU6; **D**) and GDP-bound $KRAS^{A146T}$ (PDB ID: 6BOF; **E**) showing allele-specific structural changes in the switch-I and switch-II regions, respectively. Mutated residues (green) are shown in ball and stick representation. The $KRAS^{G12R}$ mutation causes structural changes in switch-II that disrupt binding to the effector PI3Kα (**D**). The $KRAS^{A146T}$ mutation causes a marked extension of the switch-I region away from the nucleotide binding site that results in a high rate of nucleotide exchange (**E**). **F,** Crystal structure of GDP-bound $KRAS^{G12C}$ in complex with covalent inhibitor sotorasib (PDB ID: 6OIM). Sotorasib (green) covalently bound to C12 is shown in ball and stick representation.

first structural model of RAS was based upon the structure of the GTP-binding domain of EF-Tu, an elongation factor involved in protein synthesis (3). Only a few years later, crystal structures of HRAS bound to GDP were solved, confirming that RAS, like the EF-Tu G-domain, contains a similar central β-sheet comprised of six β-strands that are surrounded by five α-helices (4). Subsequently, comparison of the structure of GDP-bound HRAS with that of HRAS bound to GppNHp, a nonhydrolyzable analogue of GTP, revealed that the tertiary structure of GDP- and GTP-bound RAS were similar, except for conformational differences observed in two regions of the protein that were designated switch-I and switch-II (5). In the years that followed, numerous structures of RAS in complex with GAPs, GEFs, and effector proteins have been solved, and in all cases, these two switch regions have been found to play an essential role in orchestrating key protein interactions (Fig. 1A). More specifically, structural analyses of RAS proteins in complex with the RAS-binding or RAS-association domains of effectors demonstrated that the switch-I region (residues 30–38) is vital for RAS-effector recognition, whereas residues in the switch-II region (residues 60–76) contribute primarily to regulatory interactions with RAS GEFs and GAPs.

POSTTRANSLATIONAL MODIFICATIONS AND RAS RECRUITMENT TO THE MEMBRANE

For many years, it has been known that localization of RAS proteins to the plasma membrane is required for their signaling function and that membrane recruitment is mediated by lipid modifications occurring at the C-terminus of the HVR. All RAS proteins are farnesylated on the cysteine residue in the C-terminal CAAX motif (where C is cysteine, A is usually an aliphatic residue, and X is any amino acid), which occurs through a multistep process that involves prenylation, proteolysis, and methylation. HRAS, NRAS, and KRAS4A are also palmitoylated on one or two cysteines found immediately upstream of the CAAX motif. In contrast, KRAS4B lacks cysteine residues for palmitoylation and instead contains a polybasic region, consisting of multiple lysine residues that promote membrane binding by interacting directly with the negatively charged headgroups on membrane lipids. Moreover, unlike other RAS family members, which traffic through the Golgi apparatus to reach the plasma membrane, KRAS4B is routed directly from the endoplasmic reticulum to the plasma membrane, and its transfer to the membrane is facilitated by PDEδ, a trafficking chaperone for prenylated proteins (6). Structural studies of KRAS4B in complex with PDEδ have shown that the interaction with PDEδ is driven by KRAS4B C-terminal residues, with farnesylated and methylated C185 of the CAAX motif binding tightly to the central hydrophobic pocket of PDEδ to allow transit of fully processed KRAS4B through the cytosol (Fig. 1B; ref. 7).

In addition to the HVR, the conserved N-terminal G-domain also plays a role in orienting RAS at the membrane surface. Previous studies have indicated that RAS G-domains can populate a few distinct orientations at the plasma membrane and that orientation preferences can be modulated by the lipid environment, nucleotide binding, as well as the presence of disease-associated mutations (8–12). In addition, RAS proteins can diffuse laterally at the plasma membrane to form higher-order oligomers called nanoclusters, with each cluster consisting of 6–7 RAS proteins (13). These RAS nanoclusters are dynamic assemblies and act as exclusive sites for effector recruitment (14). On the basis of *in vitro* and cellular data, multiple studies have suggested the existence of RAS dimers that are formed via interfaces involving helices α4/α5 or α3/α4 or, alternatively, by β2/switch-I (recently reviewed in ref. 14). One report in the past year has proposed that binding of RAS to its effector RAF may facilitate dimerization of the RAS G-domains through an allosteric mechanism that involves the galectin scaffolds (15). In a second report, it has been proposed that RAS proteins assemble into higher-order helical complexes, referred to as signalosomes, in which only some of the RAS members directly contact the plasma membrane (16). Although further studies are needed to address these models, it is clear that a more comprehensive understanding of RAS organization at the membrane will provide valuable information relevant to effector engagement and downstream signal transduction.

Like many cellular proteins, KRAS (and likely the other RAS isoforms) has been found to undergo cleavage of the initiator methionine and acetylation of the nascent N-terminus (17, 18). Structural studies of KRAS proteins lacking one or both of these modifications together with biochemical experiments have revealed that N-acetylation after removal of the initiator methionine stabilizes the tertiary structure of KRAS and is critical for retaining Mg^{2+} in the nucleotide-binding pocket. In addition, other conditional, posttranslational modifications have been reported for RAS proteins, including mono- and diubiquitination, phosphorylation, sumoylation, acetylation, and nitrosylation (19–22). Less is known regarding the regulatory effects of these posttranslational modifications; however, they likely contribute to RAS signaling dynamics and have been recently reviewed elsewhere (23).

RAS MUTATIONS AND ALLELE-SPECIFIC DIFFERENCES

Mutations in *RAS* are estimated to be responsible for approximately 20% of all human cancers (24). Among the three *RAS* genes, mutations in *KRAS* are responsible for 75% of RAS-driven cancers, followed by mutations in *NRAS* (17%) and *HRAS* (7%; ref. 24). Strikingly, the mutational frequency observed in the *RAS* genes varies significantly among different cancer types, with *KRAS* mutations predominating in pancreatic ductal adenocarcinomas, colorectal cancers, and lung adenocarcinomas. However, *NRAS* mutations are mainly observed in hematopoietic tumors and malignant melanomas, and *HRAS* mutations are most frequently detected in head and neck squamous cell carcinomas and bladder tumors. For all RAS proteins, oncogenic mutations occur primarily in the G-domain at conserved amino acid positions G12, G13, and Q61 (Fig. 1C). Distinct differences in the mutational frequency at these positions are also observed among the various RAS isoforms. For example, G12 mutations comprise 83% of all KRAS alterations, followed by G13 (14%), and Q61 (2%) mutations. In contrast, Q61 is the predominant site mutated in NRAS, followed by G12 and G13,

whereas in HRAS, a more equivalent mutational frequency of G12, G13, and Q61 is observed.

Early structural studies revealed that mutation of any of these three G-domain residues alters RAS structure in a manner that impedes GAP binding and prevents the critical "arginine finger" of the GAPs from extending into the RAS active site to promote GTP hydrolysis (25, 26). As a result, the RAS mutants remain in the active GTP-bound signaling state. More recently, studies have shown that different amino acid substitutions at a specific position can generate mutant RAS proteins with distinct biochemical, structural, and signaling properties, indicating that not all *RAS* mutations are created equal (27, 28). The structural determination of numerous oncogenic KRAS mutants have provided a more sophisticated and in-depth understanding of how specific mutations alter the regulation and function of RAS to drive tumorigenesis. These studies have revealed differences not only in the GAP-mediated and intrinsic GTPase activity of RAS, but also in GEF-mediated and intrinsic nucleotide exchange rates and in effector interactions. For example, while the G12, G13, and Q61 mutations broadly result in the loss of GAP-mediated GTPase activity, Q61 mutations also reduce the intrinsic GTPase activity of RAS, and the G13D mutation causes increased intrinsic nucleotide exchange. Interestingly, structures of $KRAS^{G13D}$ in complex with the RASGAP domain of NF1 have indicated that in contrast to substitutions at G12 and Q61, the G13D mutation allows the arginine finger of NF1 to enter the catalytic pocket for NF1-mediated GTP hydrolysis (29). Further experimentation revealed that $KRAS^{G13D}$ was uniquely sensitive to the GAP activity of NF1 but not RASA1/p120GAP and was still responsive to upstream signals when NF1 was present (29). This finding provides insight as to why a retrospective study found that patients with colorectal cancer whose tumors expressed $KRAS^{G13D}$ exhibited a responsiveness to the EGFR inhibitor, cetuximab (30). Although a dedicated prospective trial failed to support the retrospective results (31), two subsequent studies have reported that colorectal cancer cell lines expressing the G13D mutant are sensitive to EGFR inhibition and that NF1 plays a critical role in determining drug sensitivity (29, 32). Further establishing the relationship between NF1 and G13D mutants, analysis of cancer genome databases indicates that inactivating mutations in NF1 frequently co-occur in tumors expressing $KRAS^{G13D}$ alleles, whereas NF1 mutations are rarely observed in cancers expressing $KRAS^{G12}$ or $KRAS^{Q61}$ mutants (29).

With regard to KRAS, G12D and G12V are in general the most common alterations observed in human cancer. Notably, the G12R mutation, which also affects G12, is rarely observed in most cancers; however, in pancreatic ductal adenocarcinoma (PDAC), $KRAS^{G12R}$ is the third most prevalent mutation (~20%). Recent results have revealed that in PDAC, the $KRAS^{G12R}$ mutant is functionally distinct from the more common G12D and G12V mutants, in that G12R does not drive macropinocytosis, a nutrient-scavenging metabolic process needed for PDAC growth (33). Structural and biochemical analysis of the $KRAS^{G12R}$ variant found that this mutation causes perturbations in the switch-II region (Fig. 1C and D) that disrupt binding interactions with PI3Kα, a key effector required for KRAS-dependent macropinocytosis. Further analysis of KRAS-mutant PDAC lines indicated that G12R-mutant lines depend on the upregulation of PI3Kγ for macropinocytosis (33).

The A146T mutation is the fourth most common *KRAS* alteration (Fig. 1), and it is frequently observed in colorectal and hematopoietic cancers. Structural analysis of $KRAS^{A146T}$ showed that this mutation causes a marked extension of the switch-I region away from the nucleotide-binding site (Fig. 1C and E), thus promoting a high rate of intrinsic and GEF-mediated nucleotide exchange (34). Therefore, due to the ten-fold higher concentration of GTP versus GDP in the cellular milieu, this mutant exists primarily in a GTP-bound state even though it is sensitive to GAP-mediated GTP hydrolysis. Thus, in contrast to the predominant G12, G13, and Q61 mutations, the A146T mutation promotes the formation of KRAS-GTP by increasing the forward rate of GDP-to-GTP nucleotide exchange rather than conferring resistance to GAP activity (34).

RAS A59 mutations (A59T/E) also occur with low frequency in human cancer, and reports have suggested that autophosphorylation of the A59T mutant or expression of the phosphomimetic A59E accounts for the oncogenic potential of these alleles. Recently, a study has found that A59T/E mutations alter the structure of the RAS-active site to enhance intrinsic nucleotide exchange and inhibit GTP hydrolysis (Fig. 1C), and that they do so at the expense of certain effector interactions (35).

Finally, the G12C mutation, which has been observed in KRAS, NRAS, and HRAS proteins, is distinctive among all RAS alterations in that the presence of the mutationally generated cysteine residue with its thiol group provides a unique molecular handle that can be covalently modified. Previously, RAS proteins were considered undruggable due to the subnanomolar binding affinity of GDP/GTP and the lack of drug-binding pockets on the surface of RAS. However, because the G12C mutant, unlike other G12 mutants, undergoes rapid GTP–GDP cycling, it was found that thiol-reacting, small-molecule inhibitors could be used to target and trap G12C mutants in the inactive GDP-bound state (36). Due to the high prevalence of $KRAS^{G12C}$ mutations in lung adenocarcinomas, a number of inhibitors have been developed that bind covalently to cysteine 12 within the switch-II pocket of GDP-bound $KRAS^{G12C}$ (Fig. 1F). In preclinical studies, these inhibitors have been shown to disrupt oncogenic signaling and cause potent tumor regression in patient-derived xenograft models of G12C cancers (37–40). Among several $KRAS^{G12C}$ inhibitors, sotorasib and adagrasib have shown promising results in early clinical trials (41), and the FDA has recently approved sotorasib as a treatment therapy for patients with non–small cell lung cancer (NSCLC) whose tumors harbor the $KRAS^{G12C}$ mutant.

THE RAF KINASES–ESSENTIAL EFFECTORS OF RAS

In order for all RAS proteins to promote tumorigenesis, they must engage the ERK/MAPK cascade, comprised of the RAF, MEK, and ERK protein kinases (reviewed in refs. 1, 2). The initiating kinases in this effector cascade are members of the RAF kinase family, CRAF/RAF1, BRAF, and ARAF, all of which possess a RAS-binding domain (RBD) that enables

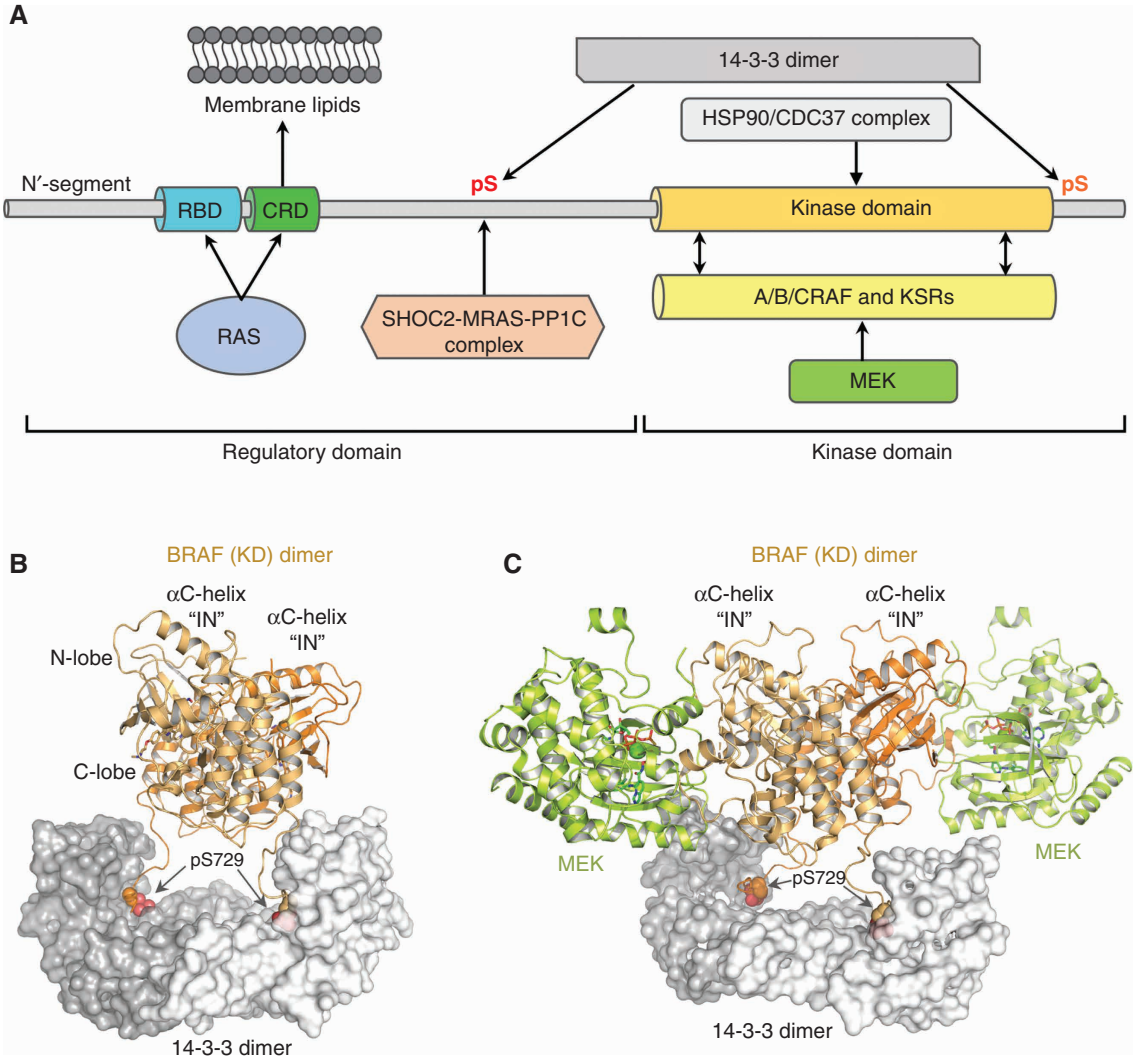

Figure 2. RAF-interacting proteins and structures of active $BRAF_2$:14-3-3_2 and $BRAF_2$:14-3-3_2:MEK_2 complexes. **A,** In the active state, the RBD and CRD present in the amino-terminal regulatory region of RAF interact with RAS, and the CRD also interacts with membrane lipids. RAF kinases contain two phosphoserines that serve as binding sites for a 14-3-3 dimer. One of these phosphoserines is located in the linker region between the CRD and the kinase domain, and the second is present in the short C-terminal tail following the kinase domain. During the RAF activation process, dephosphorylation of the phosphoserine located in the N-terminal domain is carried out by the SHOC2–MRAS–PP1C complex. The C-terminal kinase domain has been shown to homo- or heterodimerize with the kinase domains of other RAF and KSR proteins. MEK has also been found to associate with the BRAF kinase domain in the autoinhibited and active states. RAF kinases, especially CRAF/RAF1, are dependent on the HSP90/CDC37 chaperone complex for proper protein folding. **B** and **C,** The cryo-EM structures of active BRAF homodimers observed in the active $BRAF_2$:14-3-3_2 (PDB ID: 7MFF; **B**) and $BRAF_2$:14-3-3_2:MEK_2 (PDB ID: 6Q0J; **C**) complexes. Two BRAF kinase domains (light and dark orange in cartoon representation) form back-to-back dimer, with each BRAF kinase domain binding to MEK (light green in cartoon representation). A 14-3-3 dimer (light and dark gray in surface presentation) binds to the p729 sites located in the C-terminal tail of both BRAF kinase domain protomers. The BRAF regulatory domain is not visible in the cryo-EM maps of active BRAF complexes, likely due to the flexibility of these regions in the absence of membrane-binding partners.

them to interact directly with GTP-bound RAS (42, 43). The interaction with RAS promotes RAF catalytic activation, allowing RAF to phosphorylate and activate MEK, which in turn phosphorylates and activates ERK. Once activated, ERK can then phosphorylate targets throughout the cell that ultimately bring about the biological changes needed for cell proliferation and tumor growth (44). For the MEK and ERK kinases, the activation mechanism is quite straightforward with the activating phosphorylation sites located in a region of the kinase domain known as the activation segment, which undergoes a conformational change when phosphorylated that opens the catalytic site for substrate phosphorylation. In contrast, the mechanisms regulating RAF activation are much more complex, involving changes in subcellular localization, protein, and lipid interactions, as well as alterations in the RAF phosphorylation state.

All members of the RAF kinase family can be divided into two functional domains, an N-terminal regulatory domain and a C-terminal kinase domain (Fig. 2A; ref. 45). The regulatory domain contains a variable length N-terminal segment, followed by the RBD, a zinc finger–containing, cysteine-rich domain (CRD), and a linker region possessing

a phosphorylation-dependent 14-3-3 binding site (42, 43). In addition, all RAF kinases contain a second phosphorylation-dependent 14-3-3 binding site located in the short C-terminal tail that follows the kinase domain. It is important to note that members of the 14-3-3 family (β, γ, ε, σ, ζ, τ, and η in mammals) are specific phosphoserine/phosphothreonine (pS/T) binding proteins that contribute to the regulation of many cellular proteins in addition to the RAF kinases (46). They exist in cells as obligate homo- or heterodimers, with each protomer in the dimer containing an independent pS/T binding channel (47).

In quiescent cells, the RAF kinases localize to the cytosol as monomers (48), where they are maintained in a presignaling, inactive state through multiple regulatory mechanisms, including autoinhibitory contact between the RAF regulatory and kinase domains, phosphorylation of negative regulatory sites, and binding of a 14-3-3 dimer. A seminal breakthrough in understanding RAF activation came with the early discovery that the RAFs selectively interact with active GTP-bound RAS (49–51) and that the ability to bind RAS is typically a requirement for RAF activation (52). A second major advance in elucidating how the RAFs become activated enzymes emerged from crystal structures of BRAF kinase domains bound to ATP-competitive RAF inhibitors, showing that the BRAF kinase domains form back-to-back dimers (53). Subsequent mutational analysis of the 14-3-3 binding sites and key conserved residues in the RAF dimer interface and the RBD further demonstrated that dimer formation and binding of 14-3-3 to the RAF C-terminal site are needed for RAS-dependent RAF activation and that RAS binding is usually a prerequisite for the assembly of active, dimeric RAF-14-3-3 complexes (54–58). Recently, important new insight regarding the RAF activation cycle has come from cryo-electron microscopy (cryo-EM) and crystal structures of inactive and active BRAF complexes and from RAS-bound RAF complexes, providing visual context to the knowledge obtained through years of biochemical and cell-based research.

ACTIVE BRAF DIMER COMPLEXES

Because BRAF is an important driver in human cancer, many crystal structures of isolated BRAF kinase domains have been obtained. However, a 2019 study from Kondo and colleagues (59) was the first to report a cryo-EM structure of the full-length, active $BRAF_2$:14-3-3_2 complex at 3.9 Å (Fig. 2B). As expected, the BRAF kinase domains formed a back-to-back dimer, and both protomers were in a conformation that is typical for active kinases. Like other protein kinase domains, the RAF kinase domain is comprised of an N-terminal lobe (N-lobe) and a C-terminal lobe (C-lobe) that are connected by a flexible hinge region. In the active conformation, spatially conserved, hydrophobic residues spanning both the N- and C-lobes align to form two parallel columns, known as the regulatory and catalytic spines (R-spine and C-spine, respectively; ref. 60). Alignment of the spines stabilizes the lobes and orients key catalytic residues into position for substrate phosphorylation. One of the RAF R-spine residues is a leucine in the N-lobe αC-helix (L505 in BRAF), and for the R-spine to align, the αC-helix bearing this leucine residue must move to what is termed the "IN" position. In addition, this R-spine leucine lies adjacent to an arginine residue (R506 in BRAF) that plays a critical role in dimer formation and is part of the conserved RTKR (Arg-Thr-Lys-Arg) dimer interface motif (61). As a result, when the RAF kinase domains dimerize, the αC-helix shifts to the "IN" position, thereby aligning the regulatory spine and linking dimerization to catalytic activation (56).

In the cryo-EM structure reported by Kondo and colleagues (59), the αC-helices of both protomers are found in the active "IN" position with the R-spines aligned. Not unexpected, no structural density beyond the BRAF kinase domain was obtained from the full-length, active $BRAF_2$:14-3-3_2 complex, indicating that in the absence of binding partners at the plasma membrane, protein domains within the BRAF regulatory region are highly flexible. Nonetheless, this important structure was the first to demonstrate that a single 14-3-3 dimer can bridge two proteins, and for BRAF, binding to the C-terminal sites in both protomers stabilizes the dimerized kinase domains. Surprisingly, an asymmetric orientation was observed between the dimerized BRAF kinase domains and the 14-3-3 dimer, despite the fact that both dimers exhibit 2-fold symmetry. Initially, this asymmetric orientation was thought to be related to the observation that residues in the BRAF C-tail segment (residues F743-A749) of one protomer appeared to insert into the active site of the second protomer, which would block the catalytic activity of the second protomer. This configuration was also proposed to represent a transactivation mechanism similar to the "paradoxical activation" observed when a RAF inhibitor binds to one protomer in a dimer and promotes the activation of the adjacent "inhibitor-free" protomer (62). However, subsequent structures of active BRAF dimers and further biophysical studies have argued against this model. In particular, later studies have shown that both protomers can assume an active conformation with full kinase activity in the absence of the C-tail segment and that both active sites are available for occupancy even when the C-tail segment is present (63, 64). Moreover, an asymmetric orientation between the BRAF and 14-3-3 dimers has been observed in all subsequent cryo-EM and crystal structures of dimeric $BRAF_2$–14-3-3_2 complexes regardless of whether the C-tail is present or not (63–66). Interestingly, the relative orientations between the dimerized BRAF kinase domains and the 14-3-3 dimer does vary between the different structures and can be further influenced depending on whether MEK, the downstream substrate of RAF, is bound to one or both of the BRAF kinase domains (Fig. 2C). Thus, these findings suggest a flexible linkage between the BRAF and 14-3-3 dimers, which may be needed to accommodate movement within the complex generated by substrate binding and enzyme catalysis.

AUTOINHIBITED BRAF MONOMER COMPLEXES

Over the years, much less has been known regarding the structure of inactive RAF monomers. However, the groundbreaking 4.1 Å structure of a BRAF:14-3-3_2:MEK complex reported by Park and colleagues (65) changed that, revealing the domain organization and key binding partners that contribute to the RAF autoinhibited state (Fig. 3A). This structure

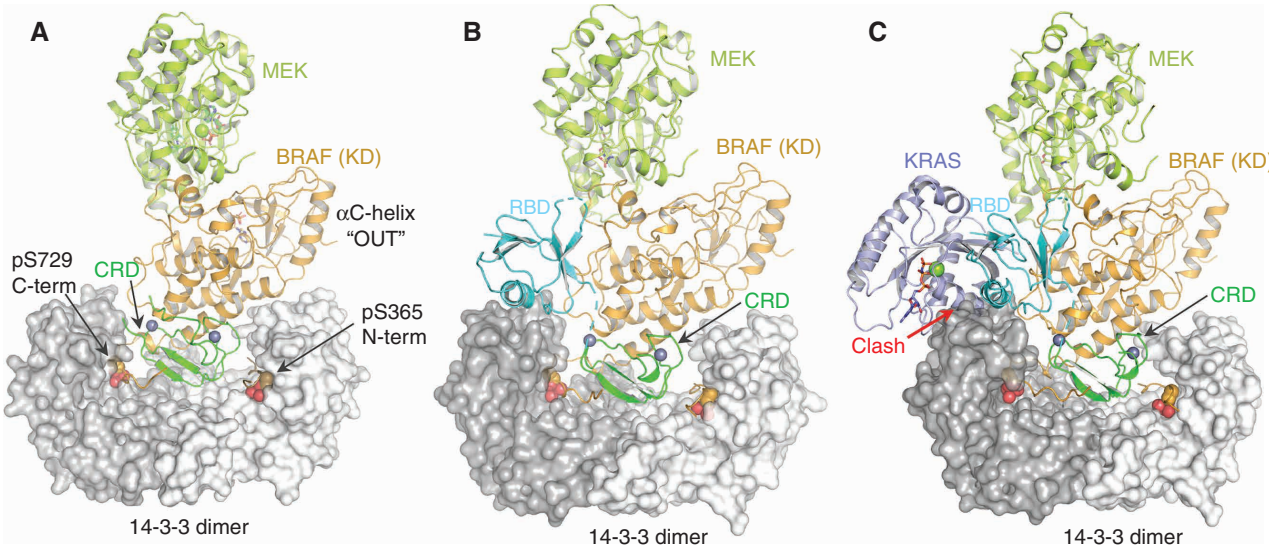

Figure 3. Structures of autoinhibited monomeric BRAF:14-3-3_2:MEK complexes. The cryo-EM structures of autoinhibited BRAF:14-3-3_2:MEK complexes with CRD (PDB ID: 6NYB; **A**) and RBD-CRD (PDB ID: 7MFD; **B**) visible in the cryo-EM reconstruction. In the autoinhibited complex, the CRD (green) is located at the center of the 14-3-3 dimer cradle and makes contacts with the 14-3-3 dimer, the BRAF kinase domain, and both the pS365 and pS729 regulatory sites. **C,** KRAS (from KRAS: RAF1 RBD structure PDB ID: 6VJJ, colored in blue) modeled onto the BRAF:14-3-3_2:MEK complex with the RBD-CRD, showing that KRAS binding to the exposed RBD would generate steric clashes (indicated by red arrow) with the 14-3-3 protomer that lies underneath the RBD. The color-coding scheme in these figures is the same as used in Fig. 2C.

firmly established that BRAF and MEK can exist in a preassembled complex prior to signaling events and confirmed the central role that 14-3-3 dimer binding and the BRAF CRD play in RAF autoinhibition. Importantly, this structure demonstrated that a 14-3-3 dimer could engage simultaneously with the BRAF N-terminal (pS365) and C-terminal (pS729) binding sites, and in doing so, occlude key regions of BRAF required for RAF dimerization and kinase activation. In particular, the 14-3-3 protomer bound to the BRAF N-terminal pS365 site was found to obstruct the dimer interface region of the BRAF kinase domain by directly contacting residues within the dimer interface (H510, D565, and Y566 of BRAF). Likewise, two loops of the BRAF CRD, which are predicted to mediate interactions with the plasma membrane (residues 240–246 and 253–260), were also occluded by 14-3-3. In the monomeric BRAF structure, the CRD sits at the center of the 14-3-3 dimer cradle, interacting with both 14-3-3 protomers and forming contacts with BRAF residues in the 14-3-3 binding motifs as well as the C-lobe of the BRAF kinase domain (Fig. 3A). The integral position of the CRD and its network of interactions within the complex are consistent with previous studies demonstrating the importance of the CRD in mediating autoinhibitory interactions (67–70). In addition, this finding provides critical insight as to why the CRD is a hotspot for germline *BRAF* mutations that upregulate ERK cascade signaling in the RASopathy developmental syndromes (71).

Although no structural information was obtained for the BRAF N-terminal segment and linker regions connecting the CRD, the pS365 site, and the kinase domain, the autoinhibited BRAF structure did reveal that the active site of the BRAF kinase domain is oriented away from the 14-3-3 dimer and contacts MEK in a face-to-face manner with juxtaposed active sites. Extensive interactions were observed between the MEK and BRAF kinase domains, with the primary points of contact being the activation segments of both kinases and their respective αG-helices, a structural element involved in kinase-substrate binding. As expected, both the MEK and BRAF kinase domains were in the inactive conformation with the αC-helices in the "OUT" position. For BRAF, the outward shift of the αC-helix was further reinforced by residues in the activation segment (residues 598–602) that form a helix-like turn, named the "inhibitory turn," which packs against hydrophobic residues in the αC-helix, the glycine-rich P loop, and the β3 strand to stabilize the inactive conformation.

In the full-length, monomeric BRAF structure reported by Park and colleagues (65), ATP-γ-S (a nonhydrolyzable ATP analogue) was bound to the active site, and the N- and C-lobes of the kinase domain were in a closer orientation than previously observed in structures of RAF inhibitor–bound kinase domains (62). A similar compact configuration of the N- and C-lobes is also observed in a 2.9 Å crystal structure of an isolated BRAF kinase domain in complex with MEK and the ATP analog AMP-PCP (ACP; ref. 66). Further analysis of this crystal structure indicates that ACP forms multiple interactions within the kinase domain that consolidate a cluster of hydrophobic residues, thereby shifting the N-lobe to this closer orientation with the C-lobe. Strikingly, in this compact configuration, key residues in the RAF dimer interface are in an unfavorable position to form and maintain the antiparallel N- to C-lobe contacts that are required for dimerization, a finding consistent with reports that ATP binding can cause the dissociation of dimers formed from isolated BRAF kinase domains (66, 72, 73). Thus, in the autoinhibited state, not only is the dimer interface obscured, it is also in a configuration that would not be conducive for

dimerization. Importantly, studies examining dimeric BRAF kinase domain:14-3-3 complexes have found that binding of the 14-3-3 dimer is required for RAF activation in that it allows the kinase domains to remain dimerized even in the presence of ATP (66). Interestingly, many of the residues central to the ACP interaction network are sites where oncogenic mutations occur, suggesting that these mutations, like 14-3-3 binding, counteract the dimer destabilizing effect of ATP.

RAS–RBD BINDING IN THE CONTEXT OF THE AUTOINHIBITED BRAF MONOMER COMPLEX

Recent cryo-EM structures of two distinct monomeric BRAF complexes at 3.7 and 4.1 Å have further confirmed the structural organization of the autoinhibitory conformation, demonstrating the importance of the BRAF CRD, the compact configuration of the BRAF kinase domain, and 14-3-3 binding in maintaining BRAF in an inactive state (64). However, in the structures of these complexes, which were isolated from a human HEK293 cell line stably expressing a tagged BRAF construct, one of the complexes contained MEK, whereas the other was "MEK-free." These findings are in agreement with previous MEK immunodepletion experiments showing that when MEK is immunodepleted from lysates of cells such as HEK293 or HCT116, significant levels of BRAF still remain, suggesting that there is a dynamic equilibrium between MEK-bound and MEK-free BRAF complexes (74). In addition, these two cryo-EM structures demonstrate that binding of the 14-3-3 dimer along with RAF inter- and intramolecular interactions are sufficient to maintain the autoinhibited conformation, albeit MEK binding may further stabilize the autoinhibited complex, as local resolution maps of the MEK-free complexes indicate an increased flexibility. Notably, a distinct feature of these monomeric BRAF structures is that the RBD was well resolved in both, revealing the orientation and position of this critical domain. In these structures, the RBD sits adjacent to the C-lobe of the BRAF kinase domain and on top of the 14-3-3 protomer bound to the pS729 site (Fig. 3B), with a large RBD:14-3-3 interface (~435 Å^2) formed by the α8-α9 helices and loop 8 of 14-3-3 and the RBD α1-helix.

Basic residues (R158, R166, K183, and R188) in the BRAF RBD that form key ionic bonds with acidic residues (E31, D33, E37, and D38) in the RAS switch-I region are largely exposed in these autoinhibited structures. However, modeling studies indicate that as RAS is engaged to form the high-affinity ionic bonds, steric clashes and electrostatic repulsion between RAS and 14-3-3 would be predicted to occur at the RBD:14-3-3 interface (Fig. 3C). In particular, residues in the RAS α1-helix and switch-I region would clash with the α8- and α9 helices of 14-3-3 that lie beneath the RBD, and electrostatic repulsion would be generated as acidic residues (D30 and E31) in RAS switch-I are brought in close proximity to acidic residues (D197 and E198) in 14-3-3. Because certain BRAF RBD residues predicted to be involved in full RAS:RBD contact (most notably, M186 and M187) are occluded by 14-3-3, Martinez Fiesco and colleagues propose that the steric clashes and electrostatic repulsion are the initiating events that instigate a change in how the 14-3-3 dimer contacts BRAF, thus exposing the occluded RBD residues (64). Moreover, mutational analysis of the RBD M186/M187 residues indicates that these methionines of BRAF are involved in RAS binding and serve a dual function, first contributing to the autoinhibited state through contact with 14-3-3 and then participating in the full spectrum of interactions with RAS that would dislodge the RBD and, in turn, the CRD, due to the short linker between these two domains, from the autoinhibited complex. Given its integral position in the autoinhibited conformation, extraction of the BRAF CRD would be predicted to facilitate the release of 14-3-3 from the pS365 site, exposing the dimer interface and allowing the pS365 site to be dephosphorylated by the SHOC2/MRAS/PP1C complex.

Finally, it should be noted that as with the autoinhibited structure reported by Park and colleagues (65), the BRAF N-terminal segment was also not resolved in the two autoinhibited structures obtained by Martinez-Fiesco and colleagues (64). However, studies utilizing bioluminescence resonance energy transfer to monitor RAS–RAF binding preferences in live cells have indicated that the RAF N-terminal segment provides an additional level of regulation in facilitating the formation of specific RAS–RAF complexes (75). In these studies, CRAF was able to bind all activated RAS proteins with high affinity, whereas BRAF exhibited preferential binding to KRAS4B that was mediated by the BRAF N-terminal segment and polybasic residues in the C-terminal, HVR of KRAS4B. Moreover, in the context of the negatively charged plasma membrane, the BRAF N-terminal segment, which carries an acidic charge and is 100–150 amino acids larger than the N-terminal segment of CRAF or ARAF, appeared to act in an inhibitory manner as removal of this region allowed BRAF to bind all RAS members with high affinity. With regard to the KRAS4B-binding preference, mutational studies support a model in which residues in the KRAS polybasic region engage acidic residues in the BRAF N-terminal segment to disrupt its inhibitory effect and permit high-affinity binding to KRAS. Although additional studies are needed to fully define the points of contact between BRAF and KRAS, these findings indicate the existence of interactions, in addition to RBD binding, that uniquely contribute to the BRAF/KRAS interaction.

RAS–RAF BINDING IS MORE THAN JUST THE RBD: INTERACTIONS WITH THE CRD

Early biochemical and structural studies established the importance of the RAF RBD in RAS binding, and although the RAF CRD was also implicated in the RAS–RAF interaction, its exact contribution has been less clear. Recently, a crystal structure of KRAS in complex with both the RBD and CRD of CRAF/RAF1 at 1.95 Å was reported, showing that these two tandem domains form one elongated structural entity where both the RBD and CRD interact extensively with KRAS (ref. 70; Fig. 4A and B). As previously reported (76, 77), the KRAS–RBD interface is formed by the KRAS switch-I region, with KRAS and the RBD interacting via their β strands to form an extended β sheet structure (Figs. 4B and C and 5A). In contrast, CRD interactions did not involve the KRAS switch regions, but instead were mediated via residues in the interswitch region (R41, K42, Q43, V44, V45, I46, D47, and G48) and helix α5 (R149, D153, and Y157; Figs. 4B, C, and 5B). Notably, the KRAS–CRD interaction interface is similar in size to the

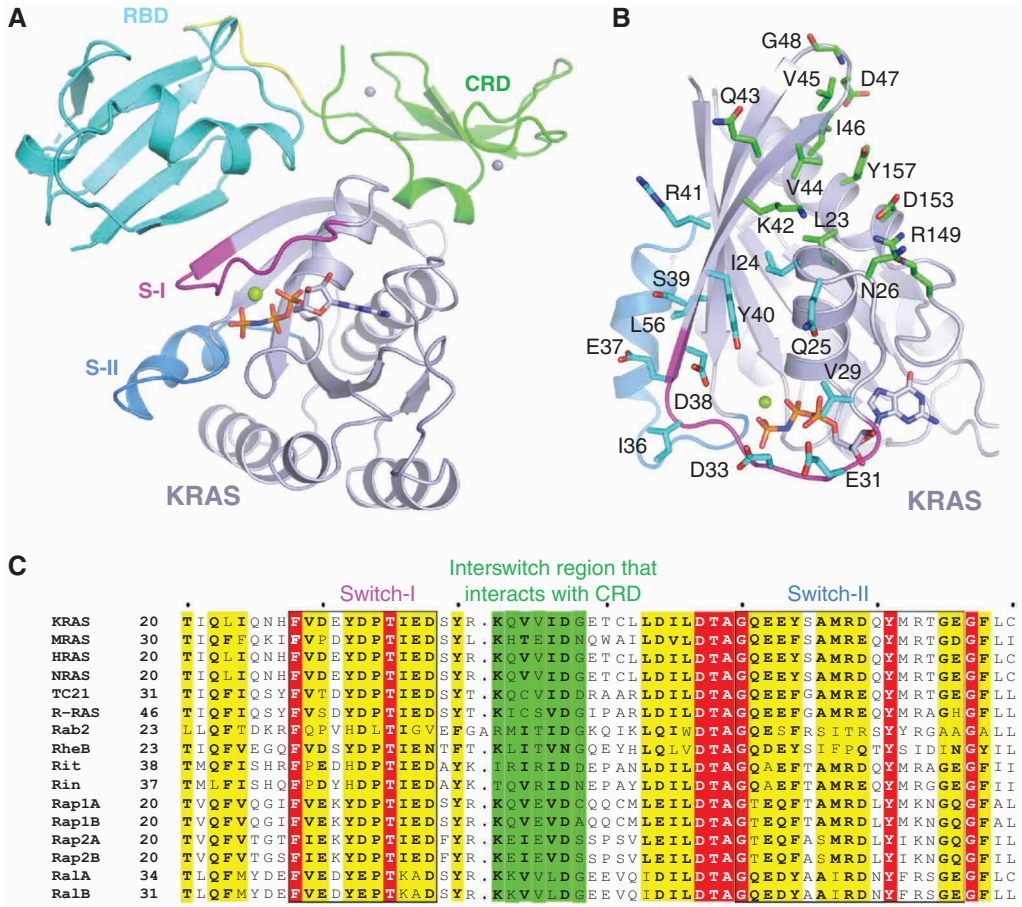

Figure 4. Structure of KRAS complexed with CRAF/RAF1 RBD-CRD and sequence analysis of RBD-CRD interacting residues in members of RAS subfamily. **A,** Crystal structure of GppNHp-bound KRAS in complex with CRAF/RAF1 RBD-CRD shown in cartoon representation (PDB ID: 6XI7). KRAS, RBD, and CRD are shown in blue, cyan, and green, respectively. Switch regions have the same color scheme as in Fig. 1. **B,** KRAS with residues interacting with the RAF RBD (cyan) and CRD (green) shown in stick representation. **C,** Sequence alignment of residues in the switch and interswitch regions in members of the RAS subfamily. Partially and fully conserved residues are highlighted in yellow and red, respectively. The switch and interswitch regions are indicated above the alignment. Residues highlighted in green show a lack of conservation in the interswitch region among RAS isoforms and other members of the RAS subfamily.

KRAS–RBD interface and contains nine hydrogen bonds. In addition, the KRAS:CRAF/RAF1(RBD-CRD) structure determined by Tran and colleagues is nearly identical to the recently reported HRAS:CRAF/RAF1(RBD-CRD) structure at 2.8 Å, indicating that all RAS isoforms are likely to interact with the CRAF/RAF1(RBD–CRD) in a similar manner (78).

Surface plasmon resonance–binding studies and mutational analysis of residues at the KRAS–CRD interface indicted that although the RBD is primarily responsible for the high-affinity interaction between KRAS and CRAF/RAF1, the presence of the CRD increases the binding affinity by two-fold (70). Moreover, proper interaction between the CRD and KRAS was found to be required for full RAF activation, as mutation of residues in either the CRD (T178A) or in the short linker between the RBD and CRD (L136A) reduced KRAS-stimulated CRAF/RAF1 kinase activity in mammalian cells by 50% (70). The importance of the RAS–CRD interaction was further indicated by the analysis of more distantly related RAS-like proteins in the RAS GTPase subfamily. The RAS superfamily consists of the RAS, RHO, RAB, ARF, and RAN subfamilies, and although members of the RAS subfamily such as MRAS, RRAS, RRAS2, RAL, RHEB, RAP1, RIT, and RIN can bind RAF, they only weakly promote RAF activation (79). Sequence comparison of these RAS subfamily GTPases with the conventional RAS family members shows high sequence homology in the switch-I region, but significant sequence divergency in the interswitch region and the C-terminal helix, which constitute the main RAS–CRD interaction interface (Fig. 4B and C; ref. 70). The lack of sequence conservation at the interaction interface is likely to result in suboptimal binding to the RAF CRD, even though contact with the RBD can be mediated by the conserved switch-I region. The sequence differences at the CRD-interacting interface provide an explanation for why these RAS subfamily GTPases cannot fully activate RAF and further support a role for the RAS–CRD interaction in the RAF activation process.

In the active RAS–RAF complex, not only does the CRD contact RAS, it is also predicted to interact with the plasma membrane via hydrophobic and basic residues found in two loops of the CRD (12, 80). Notably, despite being the smallest

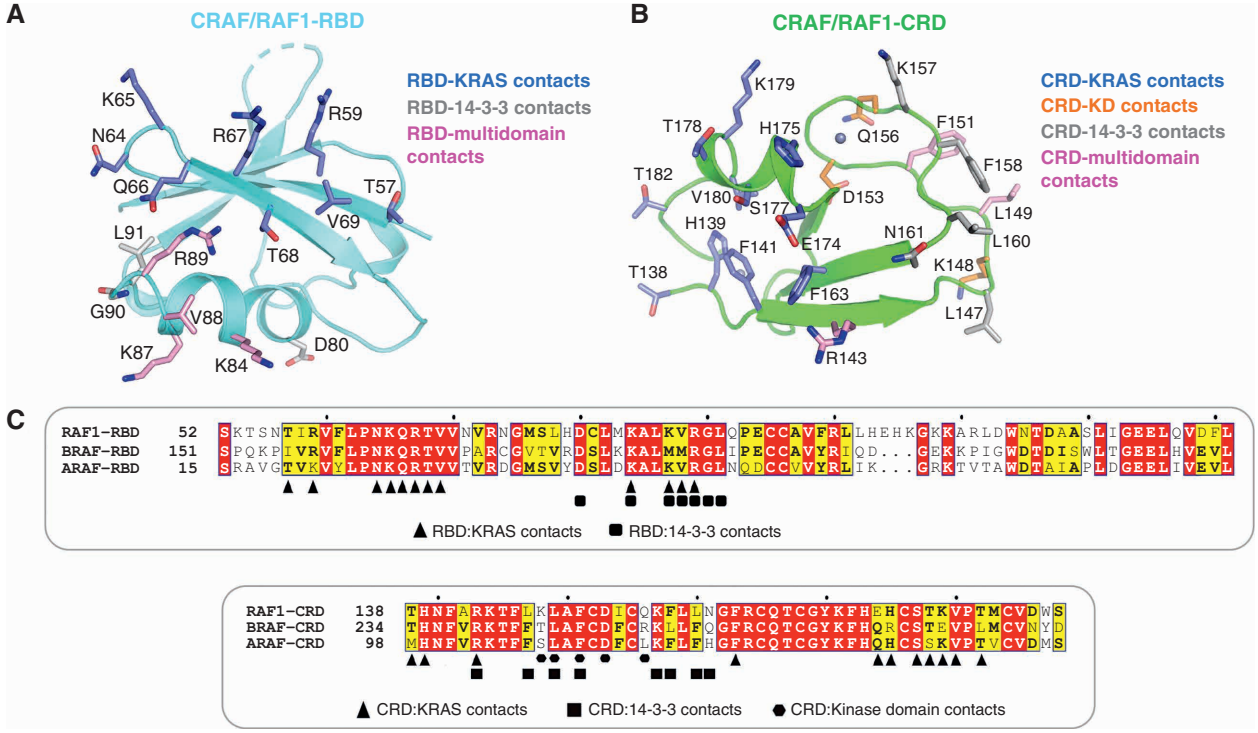

Figure 5. Mapping RBD and CRD residues involved in active and autoinhibited RAF complexes. RAF RBD (cyan; **A**) and CRD (green; **B**) are shown in cartoon representation, and residues interacting with RAS (blue), 14-3-3 (gray), and the BRAF kinase domain (orange) are shown in stick representation (PDB ID: 6XI7). Residues that interact with more than one domain or protein are colored pink. **C,** Sequence alignment of amino acids in the RBD (top) and CRD (bottom) of human CRAF/RAF1, BRAF, and ARAF. Partially and fully conserved residues among the RAF isoforms are highlighted in yellow and red, respectively. The RBD residues involved in the interaction with KRAS and 14-3-3 are indicated below the alignment with triangles and squares, respectively. Similarly, CRD residues interacting with KRAS, 14-3-3, and the RAF kinase domain are shown below the alignment with triangles, squares, and hexagons, respectively.

domain in the RAF kinases at approximately 50 amino acids, the CRD is now realized to be a critical regulatory element, interacting with 14-3-3 and the RAF kinase domain in the autoinhibited state and with RAS and the plasma membrane during the RAF activation process (Figs. 5B, C, and 6). As mentioned above, the membrane-binding loops of the CRD are occluded in the RAF autoinhibited conformation; however, CRD residues that contact KRAS are largely exposed, poised to contact RAS upon RBD binding. Together, binding interactions between RAS and the RBD and CRD at the plasma membrane would be predicted to disrupt the RAF autoinhibited state, thereby facilitating the formation of active RAF dimers.

TARGETING BRAF–MEK AND KSR–MEK COMPLEXES: INSIGHTS FROM STRUCTURAL BIOLOGY

Recent structures of RAF-containing complexes have also shed light on the mechanism of action for allosteric MEK inhibitors. In particular, high-resolution crystal structures of allosteric MEK inhibitors bound to complexes containing the isolated BRAF kinase domain and MEK have been reported, showing that as with the full-length BRAF–MEK complexes described above, the BRAF and MEK kinase domains are in the canonical inactive kinase conformation and that they interact in a face-to-face manner with juxtaposed active sites (81). Analysis of a panel of eight inhibitors revealed that despite being structurally diverse, they all bind to the previously characterized MEK allosteric site that extends along the length of the MEK activation segment helix (82, 83). The binding pocket is formed primarily by MEK; however, BRAF does make contributions in that BRAF residues N660, N661, and R662 in the pre-αG-helix loop close off one end of the pocket and BRAF-binding shapes the MEK portion of the pocket by altering the position of the MEK αC-helix as well as the activation segment helix. When bound to the pocket, all of the tested inhibitors position a polar or hydrogen bond–accepting group to interact with S212 in the MEK activation segment, thereby stabilizing the activation segment in a conformation that is resistant to RAF-mediated phosphorylation on activating sites. Of the eight allosteric MEK inhibitors studied, only two contact BRAF directly, trametinib and CH5126766/VS6766 (81), with CH5126766/VS-6766 reported to stabilize MEK and RAF in these inactive complexes (84, 85). Interestingly, structures of trametinib bound to KSR-MEK have also been reported and show that trametinib makes contacts with residues in the KSR pre-αG-helix loop (86).

The KSR proteins (KSR1 and KSR2) are members of the larger RAF kinase family, and they possess a pseudokinase domain that can bind MEK in a manner similar to the catalytically active RAF kinase domain (74). Recent structural studies of several allosteric MEK inhibitors bound to

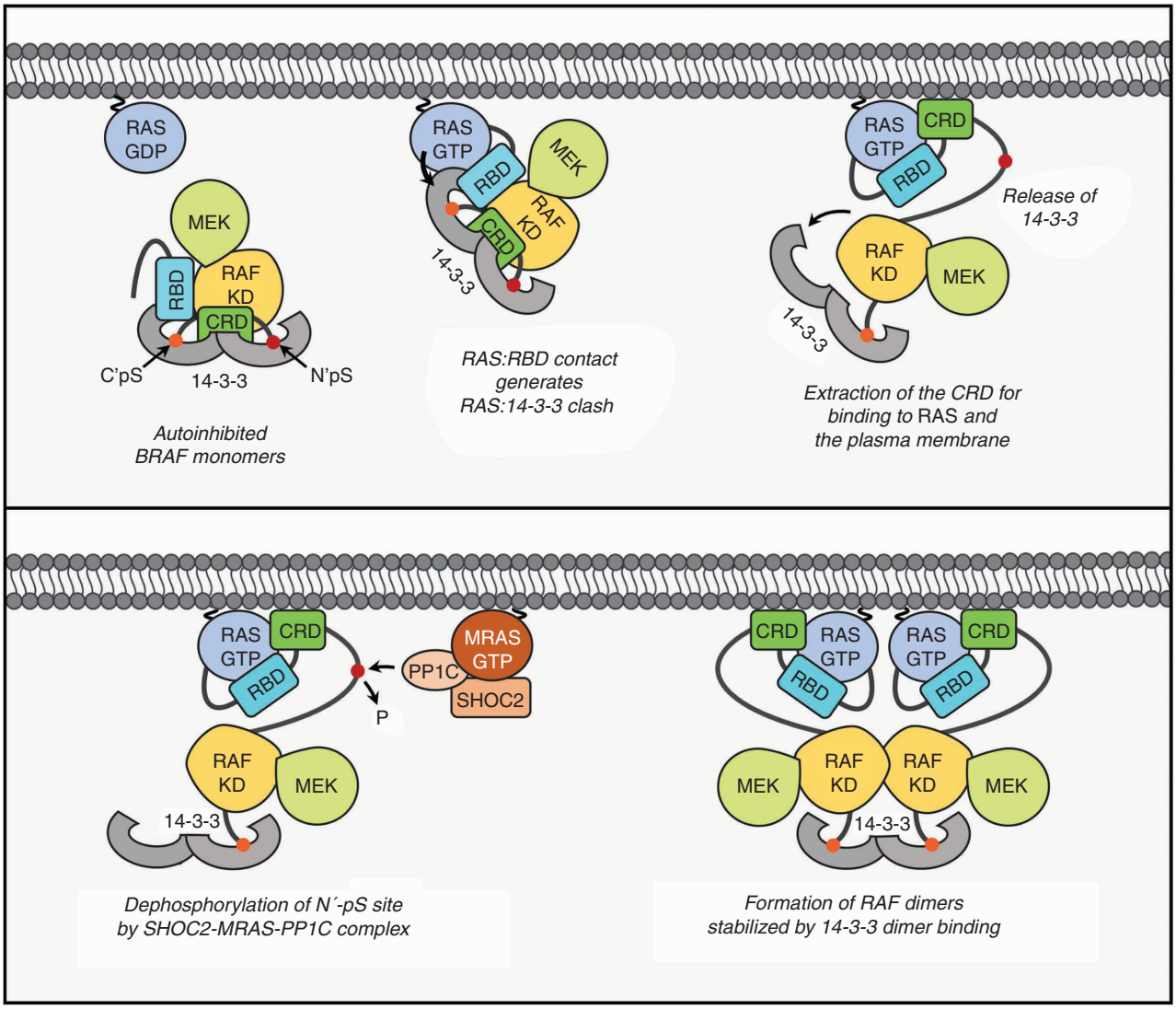

Figure 6. Model of RAS-mediated RAF activation based on the insights obtained from the recent structures of RAF complexes. RAF activation cycle starts when the switch-I region of active RAS interacts with RBD in the autoinhibited RAF complex. The formation of RAS–RAF RBD interaction causes steric clash and electrostatic repulsion between RAS and 14-3-3, resulting in conformational changes that dislodge the RBD and CRD from the autoinhibited RAF complex. This action allows the CRD to interact with the plasma membrane and RAS to further stabilize the RAS–RAF interaction. The release of the CRD promotes a rearrangement in 14-3-3 dimer binding, thus exposing the RAF dimer interface and the pS site present in the linker between the CRD and the RAF kinase domain. Dephosphorylation of this pS site by the SHOC2–MRAS–PP1C complex allows the exposed kinase domain to dimerize, forming an active dimeric RAF complex, stabilized by the binding of a 14-3-3 dimer to the pS sites located in the C-terminal tail of each RAF protomer.

complexes containing KSR and MEK have demonstrated that the inhibitor compounds also bind to the MEK allosteric pocket in these complexes, and that the presence of KSR increases the size of the pocket by modifying the position of the MEK activation segment to an extended outward conformation (86). Importantly, this remodeling of the pocket was found to impact binding affinities, kinetics, and drug residency times, with trametinib exhibiting the slowest dissociation kinetics from the KSR–MEK complexes. Together, these structural studies identify the MEK–KSR and MEK–BRAF complexes as biologically relevant targets of the allosteric MEK inhibitors. Based on these structures, next-generation allosteric MEK inhibitors are being developed that recognize specific MEK complexes as well as those that combine various properties of the current inhibitors. For example, a trametinib analogue, known as trametiglue, has been designed to retain the potency of trametinib as well as its off-rate kinetics on KSR–MEK complexes, but similar to CH5126766/VS67666, also stabilize and potentially trap BRAF–MEK complexes in the inactive state. Further work with these and other allosteric MEK inhibitors may lead to more effective treatment therapies.

UNRESOLVED ISSUES AND FUTURE DIRECTIONS

The recently determined RAS and RAF structures have significantly advanced our understanding of RAS and RAF

regulation; however, outstanding issues still remain, and the new structures themselves pose some additional questions. In particular, it is unclear whether all RAF family members will exhibit a similar autoinhibited conformation as is observed for BRAF, and little is known regarding the regulatory mechanisms that determine the formation of RAF homodimers versus heterodimers, in particular, the heterodimeric BRAF–CRAF/RAF1 complexes that predominate in RAS-driven signaling. Moreover, in the context of the plasma membrane and RAS binding, whether regions other than the RAF kinase domain make contacts that modulate the dynamics of dimerization is not known, nor is the extent to which full-length RAF dimers impact the organization of RAS complexes at the membrane.

In addition to providing key regulatory insights, these structures have also provided important new information relevant to therapeutic drug targeting. For example, with mounting structural and biochemical evidence supporting isoform and mutation-specific differences in oncogenic RAS alleles, it is becoming increasingly apparent that a single therapeutic strategy will not work for all RAS-driven cancers. Understanding and exploiting these isoform and mutation-specific differences may reveal distinct vulnerabilities, enabling the development of more refined treatment regimens for specific cancer types. In addition, the autoinhibited RAF structures have also demonstrated the potential feasibility of designing inhibitors that stabilize the inactive "compact configuration" of the RAF kinase domain by engaging not only the ATP-binding site, but also residues in the P-loop and kinase domain C-lobe to mimic ATP binding. Moreover, similar approaches to trap RAF and/or other components within the autoinhibited RAF complexes in an inactive state may prove advantageous, as is predicted for the next-generation allosteric MEK inhibitors described above. Thus, based on these initial structural studies, it is exciting to envision a multidisciplinary approach that combines structural biology with cell-based signaling analyses to spur the development of new compounds and inhibitors to combat aberrant RAS- and RAF-dependent signaling in tumor cells.

Authors' Disclosures

No disclosures were reported.

Disclaimer

The content of this publication does not necessarily reflect the views or policies of the Department of Health and Human Services, and the mention of trade names, commercial products, or organizations does not imply endorsement by the U.S. Government.

Acknowledgments

This project was funded in part with federal funds from the NCI, NIH, under contract number HHSN261200800001E (to D.K. Simanshu) and project number ZIA BC 010329 (to D.K. Morrison).

Received November 9, 2021; revised December 13, 2021; accepted December 14, 2021; published first January 19, 2022.

REFERENCES

1. Simanshu DK, Nissley DV, McCormick F. RAS proteins and their regulators in human disease. Cell 2017;170:17–33.
2. Cox AD, Der CJ. Ras history: the saga continues. Small GTPases 2010;1:2–27.
3. McCormick F, Clark BF, la Cour TF, Kjeldgaard M, Norskov-Lauritsen L, Nyborg J. A model for the tertiary structure of p21, the product of the ras oncogene. Science 1985;230:78–82.
4. Pai EF, Kabsch W, Krengel U, Holmes KC, John J, Wittinghofer A. Structure of the guanine-nucleotide-binding domain of the Ha-ras oncogene product p21 in the triphosphate conformation. Nature 1989;341:209–14.
5. Milburn MV, Tong L, deVos AM, Brunger A, Yamaizumi Z, Nishimura S, et al. Molecular switch for signal transduction: structural differences between active and inactive forms of protooncogenic ras proteins. Science 1990;247:939–45.
6. Chandra A, Grecco HE, Pisupati V, Perera D, Cassidy L, Skoulidis F, et al. The GDI-like solubilizing factor PDEdelta sustains the spatial organization and signalling of Ras family proteins. Nat Cell Biol 2011;14:148–58.
7. Dharmaiah S, Bindu L, Tran TH, Gillette WK, Frank PH, Ghirlando R, et al. Structural basis of recognition of farnesylated and methylated KRAS4b by PDEdelta. Proc Natl Acad Sci U S A 2016;113:E6766–E75.
8. Li ZL, Buck M. Computational modeling reveals that signaling lipids modulate the orientation of K-Ras4A at the membrane reflecting protein topology. Structure 2017;25:679–89.
9. Mazhab-Jafari MT, Marshall CB, Smith MJ, Gasmi-Seabrook GM, Stathopulos PB, Inagaki F, et al. Oncogenic and RASopathy-associated K-RAS mutations relieve membrane-dependent occlusion of the effector-binding site. Proc Natl Acad Sci U S A 2015;112:6625–30.
10. Abankwa D, Gorfe AA, Inder K, Hancock JF. Ras membrane orientation and nanodomain localization generate isoform diversity. Proc Natl Acad Sci U S A 2010;107:1130–5.
11. Prakash P, Zhou Y, Liang H, Hancock JF, Gorfe AA. Oncogenic K-Ras binds to an anionic membrane in two distinct orientations: a molecular dynamics analysis. Biophys J 2016;110:1125–38.
12. Fang Z, Lee KY, Huo KG, Gasmi-Seabrook G, Zheng L, Moghal N, et al. Multivalent assembly of KRAS with the RAS-binding and cysteine-rich domains of CRAF on the membrane. Proc Natl Acad Sci U S A 2020;117:12101–8.
13. Tian T, Harding A, Inder K, Plowman S, Parton RG, Hancock JF. Plasma membrane nanoswitches generate high-fidelity Ras signal transduction. Nat Cell Biol 2007;9:905–14.
14. Van QN, Prakash P, Shrestha R, Balius TE, Turbyville TJ, Stephen AG. RAS nanoclusters: dynamic signaling platforms amenable to therapeutic intervention. Biomolecules 2021;11:377.
15. Packer MR, Parker JA, Chung JK, Li Z, Lee YK, Cookis T, et al. Raf promotes dimerization of the Ras G-domain with increased allosteric connections. Proc Natl Acad Sci U S A 2021;118:e2015648118.
16. Mysore VP, Zhou ZW, Ambrogio C, Li L, Kapp JN, Lu C, et al. A structural model of a Ras-Raf signalosome. Nat Struct Mol Biol 2021;28:847–57.
17. Ntai I, Fornelli L, DeHart CJ, Hutton JE, Doubleday PF, LeDuc RD, et al. Precise characterization of KRAS4b proteoforms in human colorectal cells and tumors reveals mutation/modification cross-talk. Proc Natl Acad Sci U S A 2018;115:4140–5.
18. Dharmaiah S, Tran TH, Messing S, Agamasu C, Gillette WK, Yan W, et al. Structures of N-terminally processed KRAS provide insight into the role of N-acetylation. Sci Rep 2019;9:10512.
19. Bivona TG, Quatela SE, Bodemann BO, Ahearn IM, Soskis MJ, Mor A, et al. PKC regulates a farnesyl-electrostatic switch on K-Ras that promotes its association with Bcl-XL on mitochondria and induces apoptosis. Mol Cell 2006;21:481–93.
20. Jura N, Scotto-Lavino E, Sobczyk A, Bar-Sagi D. Differential modification of Ras proteins by ubiquitination. Mol Cell 2006;21:679–87.
21. Lander HM, Ogiste JS, Teng KK, Novogrodsky A. p21ras as a common signaling target of reactive free radicals and cellular redox stress. J Biol Chem 1995;270:21195–8.
22. Yang MH, Nickerson S, Kim ET, Liot C, Laurent G, Spang R, et al. Regulation of RAS oncogenicity by acetylation. Proc Natl Acad Sci U S A 2012;109:10843–8.

23. Campbell SL, Philips MR. Post-translational modification of RAS proteins. Curr Opin Struct Biol 2021;71:180–92.
24. Prior IA, Hood FE, Hartley JL. The frequency of Ras mutations in cancer. Cancer Res 2020;80:2969–74.
25. Ahmadian MR, Stege P, Scheffzek K, Wittinghofer A. Confirmation of the arginine-finger hypothesis for the GAP-stimulated GTP-hydrolysis reaction of Ras. Nat Struct Biol 1997;4:686–9.
26. Scheffzek K, Ahmadian MR, Kabsch W, Wiesmüller L, Lautwein A, Schmitz F, et al. The Ras-RasGAP complex: structural basis for GTPase activation and its loss in oncogenic Ras mutants. Science 1997;277:333–8.
27. Hunter JC, Manandhar A, Carrasco MA, Gurbani D, Gondi S, Westover KD. Biochemical and structural analysis of common cancer-associated KRAS mutations. Mol Cancer Res 2015;13:1325–35.
28. Haigis KM. KRAS alleles: the devil is in the detail. Trends Cancer 2017;3:686–97.
29. Rabara D, Tran TH, Dharmaiah S, Stephens RM, McCormick F, Simanshu DK, et al. KRAS G13D sensitivity to neurofibromin-mediated GTP hydrolysis. Proc Natl Acad Sci U S A 2019;116:22122–31.
30. De Roock W, Jonker DJ, Di Nicolantonio F, Sartore-Bianchi A, Tu D, Siena S, et al. Association of KRAS p.G13D mutation with outcome in patients with chemotherapy-refractory metastatic colorectal cancer treated with cetuximab. JAMA 2010;304:1812–20.
31. Segelov E, Thavaneswaran S, Waring PM, Desai J, Robledo KP, Gebski VJ, et al. Response to cetuximab with or without irinotecan in patients With refractory metastatic colorectal cancer harboring the KRAS G13D mutation: Australasian Gastro-Intestinal Trials Group ICECREAM Study. J Clin Oncol 2016;34:2258–64.
32. McFall T, Diedrich JK, Mengistu M, Littlechild SL, Paskvan KV, Sisk-Hackworth L, et al. A systems mechanism for KRAS mutant allele-specific responses to targeted therapy. Sci Signal 2019;12:eaaw8288.
33. Hobbs GA, Baker NM, Miermont AM, Thurman RD, Pierobon M, Tran TH, et al. Atypical KRAS(G12R) mutant is impaired in PI3K signaling and macropinocytosis in pancreatic cancer. Cancer Discov 2020;10:104–23.
34. Poulin EJ, Bera AK, Lu J, Lin YJ, Strasser SD, Paulo JA, et al. Tissue-Specific Oncogenic Activity of KRAS(A146T). Cancer Discov 2019;9:738–55.
35. Johnson CW, Seo HS, Terrell EM, Yang MH, KleinJan F, Gebregiworgis T, et al. Regulation of GTPase function by autophosphorylation. bioRxiv.
36. Patricelli MP, Janes MR, Li LS, Hansen R, Peters U, Kessler LV, et al. Selective inhibition of oncogenic KRAS output with small molecules targeting the inactive State. Cancer Discov 2016;6:316–29.
37. Ostrem JM, Peters U, Sos ML, Wells JA, Shokat KM. K-Ras(G12C) inhibitors allosterically control GTP affinity and effector interactions. Nature 2013;503:548–51.
38. Canon J, Rex K, Saiki AY, Mohr C, Cooke K, Bagal D, et al. The clinical KRAS(G12C) inhibitor AMG 510 drives anti-tumour immunity. Nature 2019;575:217–23.
39. Hallin J, Engstrom LD, Hargis L, Calinisan A, Aranda R, Briere DM, et al. The KRAS(G12C) inhibitor MRTX849 provides insight toward therapeutic susceptibility of KRAS-mutant cancers in mouse models and patients. Cancer Discov 2020;10:54–71.
40. Janes MR, Zhang J, Li LS, Hansen R, Peters U, Guo X, et al. Targeting KRAS mutant cancers with a covalent G12C-specific inhibitor. Cell 2018;172:578–89.
41. Van QN, Lopez CA, Tonelli M, Taylor T, Niu B, Stanley CB, et al. Uncovering a membrane-distal conformation of KRAS available to recruit RAF to the plasma membrane. Proc Natl Acad Sci U S A 2020;117:24258–68.
42. Lavoie H, Therrien M. Regulation of RAF protein kinases in ERK signalling. Nat Rev Mol Cell Biol 2015;16:281–98.
43. Terrell EM, Morrison DK. Ras-mediated activation of the Raf family kinases. Cold Spring Harb Perspect Med 2019;9:a033746.
44. Lavoie H, Gagnon J, Therrien M. ERK signalling: a master regulator of cell behaviour, life and fate. Nat Rev Mol Cell Biol 2020;21:607–32.
45. Daum G, Eisenmann-Tappe I, Fries HW, Troppmair J, Rapp UR. The ins and outs of Raf kinases. Trends Biochem Sci 1994;19:474–80.
46. Fu H, Subramanian RR, Masters SC. 14-3-3 Proteins: structure, function, and regulation. Annu Rev Pharmacol Toxicol 2000;40:617–47.
47. Gardino AK, Smerdon SJ, Yaffe MB. Structural determinants of 14-3-3 binding specificities and regulation of subcellular localization of 14-3-3-ligand complexes: a comparison of the X-ray crystal structures of all human 14-3-3 isoforms. Semin Cancer Biol 2006;16:173–82.
48. Nan X, Collisson EA, Lewis S, Huang J, Tamguney TM, Liphardt JT, et al. Single-molecule superresolution imaging allows quantitative analysis of RAF multimer formation and signaling. Proc Natl Acad Sci U S A 2013;110:18519–24.
49. Van Aelst L, Barr M, Marcus S, Polverino A, Wigler M. Complex formation between Ras and Raf and other protein kinases. Proc Natl Acad Sci U S A 1993;90:6213–7.
50. Vojtek AB, Hollenberg SM, Cooper JA. Mammalian Ras interacts directly with the serine/threonine kinase Raf. Cell 1993;74:205–14.
51. Zhang XF, Settleman J, Kyriakis JM, Takeuchi-Suzuki E, Elledge SJ, Marshall MS, et al. Normal and oncogenic p21ras proteins bind to the amino-terminal regulatory domain of c-Raf-1. Nature 1993;364:308–13.
52. Fabian JR, Vojtek AB, Cooper JA, Morrison DK. A single amino acid change in Raf-1 inhibits Ras binding and alters Raf-1 function. Proc Natl Acad Sci U S A 1994;91:5982–6.
53. Rajakulendran T, Sahmi M, Lefrancois M, Sicheri F, Therrien M. A dimerization-dependent mechanism drives RAF catalytic activation. Nature 2009;461:542–5.
54. Freeman AK, Ritt DA, Morrison DK. The importance of Raf dimerization in cell signaling. Small GTPases 2013;4:180–5.
55. Garnett MJ, Rana S, Paterson H, Barford D, Marais R. Wild-type and mutant B-RAF activate C-RAF through distinct mechanisms involving heterodimerization. Mol Cell 2005;20:963–9.
56. Hu J, Stites EC, Yu H, Germino EA, Meharena HS, Stork PJ, et al. Allosteric activation of functionally asymmetric RAF kinase dimers. Cell 2013;154:1036–46.
57. Rushworth LK, Hindley AD, O'Neill E, Kolch W. Regulation and role of Raf-1/B-Raf heterodimerization. Mol Cell Biol 2006;26:2262–72.
58. Weber CK, Slupsky JR, Kalmes HA, Rapp UR. Active Ras induces heterodimerization of cRaf and BRaf. Cancer Res 2001;61:3595–8.
59. Kondo Y, Ognjenović J, Banerjee S, Karandur D, Merk A, Kulhanek K, et al. Cryo-EM structure of a dimeric B-Raf:14-3-3 complex reveals asymmetry in the active sites of B-Raf kinases. Science 2019;366:109–15.
60. Taylor SS, Shaw AS, Kannan N, Kornev AP. Integration of signaling in the kinome: architecture and regulation of the alphaC Helix. Biochim Biophys Acta 2015;1854:1567–74.
61. Baljuls A, Mahr R, Schwarzenau I, Muller T, Polzien L, Hekman M, et al. Single substitution within the RKTR motif impairs kinase activity but promotes dimerization of RAF kinase. J Biol Chem 2011;286:16491–503.
62. Karoulia Z, Wu Y, Ahmed TA, Xin Q, Bollard J, Krepler C, et al. An integrated model of RAF inhibitor action predicts inhibitor activity against oncogenic BRAF signaling. Cancer Cell 2016;30:485–98.
63. Liau NPD, Venkatanarayan A, Quinn JG, Phung W, Malek S, Hymowitz SG, et al. Dimerization induced by C-terminal 14-3-3 binding is sufficient for BRAF kinase activation. Biochemistry 2020;59:3982–92.
64. Martinez Fiesco JA, Durrant DE, Morrison DK, Zhang P. Structural insights into the BRAF monomer-to-dimer transition mediated by RAS binding. Nat Commun 2022;13:486.
65. Park E, Rawson S, Li K, Kim BW, Ficarro SB, Pino GG, et al. Architecture of autoinhibited and active BRAF-MEK1-14-3-3 complexes. Nature 2019;575:545–50.
66. Liau NPD, Wendorff TJ, Quinn JG, Steffek M, Phung W, Liu P, et al. Negative regulation of RAF kinase activity by ATP is overcome by 14-3-3-induced dimerization. Nat Struct Mol Biol 2020;27:134–41.
67. Cutler RE Jr, Stephens RM, Saracino MR, Morrison DK. Autoregulation of the Raf-1 serine/threonine kinase. Proc Natl Acad Sci U S A 1998;95:9214–9.
68. Chong H, Guan K-L. Regulation of Raf through phosphorylation and N-terminus-C terminus interaction. J Biol Chem 2003;278:36269–76.

69. Tran NH, Wu X, Frost JA. B-Raf and Raf-1 are regulated by distinct autoregulatory mechanisms. J Biol Chem 2005;280:16244–53.
70. Tran TH, Chan AH, Young LC, Bindu L, Neale C, Messing S, et al. KRAS interaction with RAF1 RAS-binding domain and cysteine-rich domain provides insights into RAS-mediated RAF activation. Nat Commun 2021;12:1176.
71. Sarkozy A, Carta C, Moretti S, Zampino G, Digilio MC, Pantaleoni F, et al. Germline BRAF mutations in Noonan, LEOPARD, and cardiofaciocutaneous syndromes: molecular diversity and associated phenotypic spectrum. Hum Mutat 2009;30:695–702.
72. Hatzivassiliou G, Song K, Yen I, Brandhuber BJ, Anderson DJ, Alvarado R, et al. RAF inhibitors prime wild-type RAF to activate the MAPK pathway and enhance growth. Nature 2010;464:431–5.
73. Lavoie H, Thevakumaran N, Gavory G, Li JJ, Padeganeh A, Guiral S, et al. Inhibitors that stabilize a closed RAF kinase domain conformation induce dimerization. Nat Chem Biol 2013;9:428–36.
74. Haling JR, Sudhamsu J, Yen I, Sideris S, Sandoval W, Phung W, et al. Structure of the BRAF-MEK complex reveals a kinase activity independent role for BRAF in MAPK signaling. Cancer Cell 2014;26:402–13.
75. Terrell EM, Durrant DE, Ritt DA, Sealover NE, Sheffels E, Spencer-Smith R, et al. Distinct binding preferences between Ras and Raf family members and the impact on oncogenic Ras signaling. Mol Cell 2019;76:872–84.
76. Fetics SK, Guterres H, Kearney BM, Buhrman G, Ma B, Nussinov R, et al. Allosteric effects of the oncogenic RasQ61L mutant on Raf-RBD. Structure 2015;23:505–16.
77. Nassar N, Horn G, Herrmann C, Block C, Janknecht R, Wittinghofer A. Ras/Rap effector specificity determined by charge reversal. Nat Struct Biol 1996;3:723–9.
78. Cookis T, Mattos C. Crystal structure reveals the full Ras-Raf interface and advances mechanistic understanding of Raf activation. Biomolecules 2021;11.
79. Rodriguez-Viciana P, Sabatier C, McCormick F. Signaling specificity by Ras family GTPases is determined by the full spectrum of effectors they regulate. Mol Cell Biol 2004;24:4943–54.
80. Travers T, Lopez CA, Van QN, Neale C, Tonelli M, Stephen AG, et al. Molecular recognition of RAS/RAF complex at the membrane: role of RAF cysteine-rich domain. Sci Rep 2018;8:8461.
81. Gonzalez-Del Pino GL, Li K, Park E, Schmoker AM, Ha BH, Eck MJ. Allosteric MEK inhibitors act on BRAF/MEK complexes to block MEK activation. Proc Natl Acad Sci U S A 2021;118:e2107207118.
82. Fischmann TO, Smith CK, Mayhood TW, Myers JE, Reichert P, Mannarino A, et al. Crystal structures of MEK1 binary and ternary complexes with nucleotides and inhibitors. Biochemistry 2009;48:2661–74.
83. Ohren JF, Chen H, Pavlovsky A, Whitehead C, Zhang E, Kuffa P, et al. Structures of human MAP kinase kinase 1 (MEK1) and MEK2 describe novel noncompetitive kinase inhibition. Nat Struct Mol Biol 2004;11:1192–7.
84. Ishii N, Harada N, Joseph EW, Ohara K, Miura T, Sakamoto H, et al. Enhanced inhibition of ERK signaling by a novel allosteric MEK inhibitor, CH5126766, that suppresses feedback reactivation of RAF activity. Cancer Res 2013;73:4050–60.
85. Lito P, Saborowski A, Yue J, Solomon M, Joseph E, Gadal S, et al. Disruption of CRAF-mediated MEK activation is required for effective MEK inhibition in KRAS mutant tumors. Cancer Cell 2014;25:697–710.
86. Khan ZM, Real AM, Marsiglia WM, Chow A, Duffy ME, Yerabolu JR, et al. Structural basis for the action of the drug trametinib at KSR-bound MEK. Nature 2020;588:509–14.